Received: 16 July 2024 | Revised: 16 October 2024 | Accepted: 25 October 2024

DOI: 10.1002/aws2.70006

ORIGINAL RESEARCH

AWWA WATER SCIENCE

Drinking water buffer intensity simulator (BIS): Development and practical simulations

David G. Wahman | **Michael R. Schock** | **Darren A. Lytle**

United States Environmental Protection Agency, Office of Research & Development, Cincinnati, Ohio, USA

Correspondence
David G. Wahman, USEPA, 26 W. Martin Luther King Dr., Cincinnati, OH 45268, USA.
Email: wahman.david@epa.gov

Deputy Editor: Vanessa L. Speight
Associate Editor: Jeanine D Dudle

Abstract

An established body of research over many decades has identified the importance of both bulk-water and pipe scale surface microenvironment buffering to meet distribution system pH targets and reduce corrosivity toward metallic piping and components. Buffer intensity quantifies the ability of water to resist pH changes, and the greater the buffer intensity, the more resistant the water is to pH changes. To provide a practical tool for exploring buffer intensity, a buffer intensity simulator (BIS) was implemented in open-source R code, incorporating typical chemical species (e.g., carbonate and orthophosphate) that contribute to drinking water buffer intensity along with temperature and ionic strength impacts. The BIS was verified against a parallel spreadsheet implementation and is publicly available at https://github.com/USEPA/BIS. Simulations were conducted to illustrate impacts related to buffer intensity using three practical scenarios: carbonate buffering in drinking waters, temperature impacts, and free ammonia presence from chloramine use and/or source water presence.

KEYWORDS

buffer intensity, ionic strength, R code, temperature

1 | INTRODUCTION

Buffer intensity (β), also referred to as buffer capacity or buffer index (Urbansky & Schock, 2000), is a parameter that quantifies the ability of a given water chemistry to resist pH changes and is typically expressed in units of (milli)equivalent per liter per pH unit. Note that in this paper, the authors have chosen to use the term buffer intensity to parallel the presentation in Benjamin (2015).

Despite being related to familiar parameters of pH, alkalinity, and dissolved inorganic carbon (DIC), buffer intensity is a less recognizable, understood, and utilized parameter in the drinking water field. From a practical perspective, an increasing buffer intensity translates to a drinking water having a greater ability to resist pH changes brought about by chemical or microbially mediated reactions (Benjamin, 2015; Butler, 1964; Butler & Cogley, 1998; Clement & Schock, 1998; Loewenthal & Marais, 1976; Schock & Lytle, 2011; Stumm & Morgan, 1996; Weber & Stumm, 1964, 1963). In addition to determining buffer intensity at a specific pH, buffer intensity curves can be generated to visualize buffer intensity over a pH range, illustrating where a given water chemistry is an efficient buffer to resist pH changes. Practically, the amount of strong acid or strong base required to lower or raise, respectively, the pH of a given water chemistry is the area under a total buffer intensity curve between two pH values.

Because pH is a "master variable" (Stumm & Morgan, 1996) for metal solubility (Schock et al., 1995; Wahman

et al., 2021), buffer intensity provides information related to the mechanisms by which pH is derived and set in natural and drinking waters (Weber & Stumm, 1964, 1963). Multiple studies have focused on the role of buffer intensity in implementing corrosion control in drinking water as it relates to distribution systems and pH stability (Benjamin et al., 1996; Clement et al., 1998; Snoeyink & Wagner, 1996; Stumm, 1960; USEPA, 2019). Exercises such as these are sometimes critically important for planning long-term treatment programs to optimize distribution system water quality to meet multiple regulatory and operational objectives for the whole distribution system (Clement et al., 1998). When multiple water sources or treatment plants are part of a large water distribution network, buffer intensity computations can be helpful in assessing the probable impact of dilution or change in the water supply at a given water quality zone. Furthermore, when source water and treatment changes are considered, buffer intensity should be considered as part of understanding the potential changes to water quality.

In drinking water distribution systems, existing components of the pipe scales or cement mortar lining materials often supplement the aqueous phase homogeneous buffering mechanisms. The example of calcium carbonate deposits has been used to illustrate the mixed ("heterogenous") buffering mechanisms in environmental systems (Butler & Cogley, 1998; Stumm & Morgan, 1996; Weber & Stumm, 1963). However, drinking water pipe deposits can be highly varied mixtures of metal carbonates, hydroxycarbonates, phosphates, oxyhydroxides, and even some silicates; therefore, the role that such buffers would play is highly variable and system specific. Stumm and Morgan (1996) note that the capacity for buffering by the solids depends strongly on the amount of the solids, the solubility of the solid phase(s), and the rates of the chemical reactions between the water and mineral phases. Thus, distribution systems can be a long-term (e.g., days, weeks, or years) sink for acid or base input into the water, but the most significant and immediate buffering is normally provided by the homogeneous aqueous phase buffering, which is the subject of the current effort.

Implementation of the necessary calculations to determine homogeneous buffer intensity (hereafter buffer intensity) can be accomplished in spreadsheets (Kim, 2003; Urbansky & Schock, 2000), but a tailored drinking water implementation does not currently exist in a free, open-source format to allow quick exploration by drinking water practitioners (e.g., engineers, operators, regulators) on how simulated conditions (i.e., a given water chemistry or proposed process changes) impact buffer intensity. Furthermore, presentations on buffer intensity typically do not include further details on how temperature and ionic strength impact buffer intensity calculations. Therefore, the current work developed a free, open-source tool for the drinking water industry, allowing buffer intensity and associated buffer intensity curves to be determined that consider common weak acid or weak base chemical species (e.g., carbonate, orthophosphate, orthosilicate) found in finished drinking water.

Article Impact Statement
A buffer intensity simulator was implemented in open-source R code, incorporating typical chemical species (e.g., carbonate, orthophosphate) along with temperature and ionic strength impacts.

Presented herein is a detailed description of the underlying buffer intensity calculations, including incorporation of temperature and ionic strength impacts; verification of buffer intensity calculations from the R code against a parallel spreadsheet implementation; and a discussion of simulations conducted to illustrate the impacts of buffer intensity using three practical drinking water scenarios: (1) carbonate importance for representative drinking water conditions, (2) temperature impacts, and (3) free ammonia presence related to chloramine use and/or free ammonia source water presence. The developed code and associated discussion of simulation outputs provide the drinking water industry with a practical tool and reference materials to understand and determine buffer intensity.

2 | BUFFER INTENSITY SIMULATOR DEVELOPMENT

The developed code is referred to as the buffer intensity simulator (BIS), is freely available for download at GitHub (https://github.com/USEPA/BIS), and can be run locally on a computer with open-source software or shared online (e.g., https://www.shinyapps.io/).

2.1 | Buffer intensity calculations

The buffer intensity calculations were implemented in R (R Core Team, 2024) in a similar manner to that described in section 8.11 of Benjamin (2015) with the addition that the BIS was expanded to consider temperature and ionic strength impacts to the equilibria. The general equation for buffer intensity is provided as Equation 1a where the buffer intensity of chemical i (β_i) is the change in the concentration of chemical i ($d[i]$)

relative to the resulting change in pH (dpH). Using the substitution resulting from Equation 1b where two mathematical relationships ($\log_{10}x = \frac{\ln x}{2.303}$ and $d(\ln x) = \frac{dx}{x}$) were used and $\{H^+\}$ is the activity of the hydrogen ion, results in Equation 1c. Herein, note that the use of curly braces, { }, indicates chemical activity and square brackets, [ ], indicates chemical molar concentration (moles/L, M). Because buffer intensity is a conservative property, individual buffer intensity values determined for each weak acid or weak base system (e.g., water, carbonate, orthophosphate) present in a water (i.e., β_i values for each weak acid or weak base system) can be summed to determine the total buffer intensity (β_T) for a given water chemistry (i.e., $\beta_T = \sum\beta_i$). For example, at a given pH, ionic strength, and temperature, the buffer intensity contributed by orthophosphate to the total buffer intensity is not affected by the presence or absence of other weak acids or weak bases. The BIS provides output for the total buffer intensity as well as the buffer intensity for each individual weak acid or weak base system in typical units of (equivalent/L)/pH unit and (milliequivalent/L)/pH unit.

$$\beta_i = \frac{d[i]}{d\text{pH}} \tag{1a}$$

$$d\text{pH} = d(-\log_{10}\{H^+\}) = d\left(-\frac{\ln\{H^+\}}{2.303}\right) = -\frac{1}{2.303}\frac{d\{H^+\}}{\{H^+\}} \tag{1b}$$

$$\beta_i = \frac{d[i]}{-\frac{1}{2.303}\frac{d\{H^+\}}{\{H^+\}}} = -2.303\{H^+\}\frac{d[i]}{d\{H^+\}} \tag{1c}$$

From Equation 1c, contributions of buffer intensity from water (β_w, Equation 2) and monoprotic (β_{HA}, Equation 3), diprotic (β_{H_2A}, Equation 4), and triprotic (β_{H_3A}, Equation 5) weak acids were derived in Benjamin (2015) for 0 M ionic strength where $\{H^+\} = [H^+]$. In Equations 3–5, [TOTA] is the total concentration of a given weak acid system, such as carbonate (i.e., DIC) or orthophosphate (i.e., total orthophosphate). Thus, using the diprotic carbonate system as an example, [TOTA] is the sum of dissolved carbon dioxide plus carbonic acid (H_2CO_3*), bicarbonate ion (HCO_3^-), and carbonate ion (CO_3^{2-}) concentrations. The α_0, α_1, α_2, and α_3 values are the fraction of [TOTA] that is in the various forms of the weak acid species from the most protonated (α_0) to the less protonated forms (α_1, α_2, and α_3). The α equations for monoprotic (α_0 and α_1), diprotic (α_0, α_1, and α_2), and triprotic (α_0, α_1, α_2, and α_3) acids are summarized in Table 1. Continuing the diprotic carbonate example, α_0, α_1, and α_2 correspond to the fractions of DIC that are H_2CO_3*, HCO_3^-, and CO_3^{2-}, respectively.

$$\beta_w = -\frac{d[H^+]}{d\text{pH}} + \frac{d[OH^-]}{d\text{pH}} = 2.303([H^+] + [OH^-]) \tag{2}$$

$$\beta_{HA} = 2.303[\text{TOTA}](\alpha_0\alpha_1) \tag{3}$$

$$\beta_{H_2A} = 2.303[\text{TOTA}](\alpha_0\alpha_1 + 4\alpha_0\alpha_2 + \alpha_1\alpha_2) \tag{4}$$

$$\beta_{H_3A} = 2.303[\text{TOTA}]\left(\alpha_0\alpha_1 + 4\alpha_0\alpha_2 + 9\alpha_0\alpha_3 + \alpha_1\alpha_2 + 4\alpha_1\alpha_3 + \alpha_2\alpha_3\right) \tag{5}$$

To account for temperature and ionic strength impacts to equilibria that ultimately impact chemical concentrations, concentration-based equilibrium constants at the desired temperature (see *Equilibrium constants* and *Ionic*

TABLE 1 Weak acid α equation summary for monoprotic (e.g., free ammonia), dibprotic (e.g., carbonate), and triprotic (e.g., orthophosphate) weak acids.[a]

α equation	Monoprotic weak acid $[\text{TOTA}] = [HA] + [A^-]$	Diprotic weak acid $[\text{TOTA}] = [H_2A] + [HA^-] + [A^{2-}]$	Triprotic weak acid $[\text{TOTA}] = [H_3A] + [H_2A^-] + [HA^{2-}] + [A^{3-}]$
α_0	$\frac{[HA]}{[\text{TOTA}]} = \frac{1}{1+\frac{K_1}{\{H^+\}}}$	$\frac{[H_2A]}{[\text{TOTA}]} = \frac{1}{1+\frac{K_1}{\{H^+\}}+\frac{K_1K_2}{\{H^+\}^2}}$	$\frac{[H_3A]}{[\text{TOTA}]} = \frac{1}{1+\frac{K_1}{\{H^+\}}+\frac{K_1K_2}{\{H^+\}^2}+\frac{K_1K_2K_3}{\{H^+\}^3}}$
α_1	$\frac{[A^-]}{[\text{TOTA}]} = \frac{1}{1+\frac{\{H^+\}}{K_1}}$	$\frac{[HA^-]}{[\text{TOTA}]} = \frac{1}{1+\frac{\{H^+\}}{K_1}+\frac{K_2}{\{H^+\}}}$	$\frac{[H_2A^-]}{[\text{TOTA}]} = \frac{1}{1+\frac{\{H^+\}}{K_1}+\frac{K_2}{\{H^+\}}+\frac{K_2K_3}{\{H^+\}^2}}$
α_2		$\frac{[A^{2-}]}{[\text{TOTA}]} = \frac{1}{1+\frac{\{H^+\}}{K_2}+\frac{\{H^+\}^2}{K_1K_2}}$	$\frac{[HA^{2-}]}{[\text{TOTA}]} = \frac{1}{1+\frac{\{H^+\}}{K_2}+\frac{\{H^+\}^2}{K_1K_2}+\frac{K_3}{\{H^+\}}}$
α_3			$\frac{[A^{3-}]}{[\text{TOTA}]} = \frac{1}{1+\frac{\{H^+\}^3}{K_1K_2K_3}+\frac{\{H^+\}^2}{K_2K_3}+\frac{\{H^+\}}{K_3}}$

[a]Concentration corrected equilibrium constants (K_{IS}) calculated as per Table 2 are used in the α equations for K_1, K_2, and K_3 as appropriate. $\{H^+\}$ is hydrogen ion activity (10^{-pH}); [TOTA] is the total concentration of a given weak acid system; and [HA] and $[A^-]$ (monoprotic weak acid), $[H_2A]$, $[HA^-]$, and $[A^{2-}]$ (diprotic weak acid), and $[H_3A]$, $[H_2A^-]$, $[HA^{2-}]$, and $[A^{3-}]$ (triprotic weak acid) are the concentrations of individual chemical species in a given weak acid system where H is hydrogen and A is specific to the weak acid system (e.g., $A = NH_3$, $A = CO_3$, or $A = PO_4$ for the ammonia, carbonate, and phosphate systems, respectively).

strength corrections) are used in α_0, α_1, α_2, and α_3 calculations along with hydrogen ion activity ($\{H^+\} = 10^{-pH}$) in Equations 3–5. For the buffer intensity of water, an alternative derivation of Equation 2 ($\beta_{w,IS}$ from Equations 6a–6c) that uses $\{H^+\}$ and hydroxide ion activity ($\{OH^-\}$) was implemented, allowing for a simpler BIS code. In Equation 6c, γ_1 is the activity coefficient for a single charged ion (see *Ionic strength corrections*).

$$-\frac{d[H^+]}{dpH} = -\frac{d(\gamma_1\{H^+\})}{-\frac{1}{2.303}\frac{d\{H^+\}}{\{H^+\}}} = 2.303(\gamma_1)\{H^+\} \quad (6a)$$

$$\frac{d[OH^-]}{dpH} = \frac{d\left(\frac{(\gamma_1)K_w}{\{H^+\}}\right)}{-\frac{1}{2.303}\frac{d\{H^+\}}{\{H^+\}}} = \frac{-\frac{(\gamma_1)K_w}{\{H^+\}^2}d\{H^+\}}{-\frac{1}{2.303}\frac{d\{H^+\}}{\{H^+\}}} = 2.303\frac{(\gamma_1)K_w}{\{H^+\}} = 2.303(\gamma_1)\{OH^-\} \quad (6b)$$

$$\beta_{w,IS} = -\frac{d[H^+]}{dpH} + \frac{d[OH^-]}{dpH} = 2.303(\gamma_1)(\{H^+\} + \{OH^-\}) \quad (6c)$$

2.2 | Equilibria

Relevant chemical equilibria typically present in finished drinking water were selected for inclusion in the BIS (Table 2). The equilibria selected include water, carbonate because it is a naturally occuring buffer or added during drinking water treatment (e.g., lime softening, recarbonation, and caustic addition), orthosilicate because it is naturally occuring or added for corrosion control, orthophosphate because it is added for corrosion control, and weak acid or weak base chemicals associated with disinfection because they may persist during distribution (free ammonia, free chlorine, and free bromine).

TABLE 2 Summary of equilibrium and associated equilibrium constant (K) equation for a specified temperature in Kelvin (T), negative base 10 logarithm of the equilibrium constant at 25°C (298.15 Kelvin) and 0 M ionic strength (pK_{25C}), and concentration-based equilibrium constant equation (K_{IS}).

System (reference)	Equilibrium and equilibrium constant (K) equation	pK_{25C}	K_{IS}[a]
Carbonate (Plummer & Busenberg, 1982)	$H_2CO_3^* \rightleftharpoons HCO_3^- + H^+$ $\log_{10}K_{c1} = -356.3094 - 0.06091964 \times T + \frac{21,834.37}{T} + 126.8339 \times \log_{10}T - \frac{1,684,915}{T^2}$	6.352	$\frac{K_{c1}}{\gamma_1}$
	$HCO_3^- \rightleftharpoons CO_3^{2-} + H^+$ $\log_{10}K_{c2} = -107.8871 - 0.03252849 \times T + \frac{5,151.79}{T} + 38.92561 \times \log_{10}T - \frac{563,713.9}{T^2}$	10.329	$\gamma_1\frac{K_{c2}}{\gamma_2}$
Free Ammonia (Bates & Pinching, 1949)	$NH_4^+ \rightleftharpoons NH_3 + H^+$ $\log_{10}K_n = 0.6322 - 0.001225 \times T - \frac{2,835.76}{T}$	9.244	$\gamma_1(K_n)$
Free Bromine[b] (Benjamin, 2015)	$HOBr \rightleftharpoons OBr^- + H^+$ $\log_{10}K_{br} = \frac{\Delta H_r^\circ}{2.303R}\left(\frac{1}{298.15} - \frac{1}{T}\right) + \log_{10}K_{br,25C}$	8.63	$\frac{K_{br}}{\gamma_1}$
Free Chlorine (Morris, 1966)	$HOCl \rightleftharpoons OCl^- + H^+$ $\log_{10}K_{cl} = 10.0686 - 0.0253 \times T - \frac{3,000}{T}$	7.54	$\frac{K_{cl}}{\gamma_1}$
Orthophosphate[b] (Goldberg et al., 2002)	$H_3PO_4 \rightleftharpoons H_2PO_4^- + H^+$ $\log_{10}K_{p1} = \frac{\Delta H_r^\circ}{2.303R}\left(\frac{1}{298.15} - \frac{1}{T}\right) + \frac{\Delta C_p^\circ}{2.303R}\left(\frac{298.15}{T} - 1 - 2.303 \times \log_{10}\frac{298.15}{T}\right) + \log_{10}K_{p1,25C}$	2.148	$\frac{K_{p1}}{\gamma_1}$
	$H_2PO_4^- \rightleftharpoons HPO_4^{2-} + H^+$ $\log_{10}K_{p2} = \frac{\Delta H_r^\circ}{2.303R}\left(\frac{1}{298.15} - \frac{1}{T}\right) + \frac{\Delta C_p^\circ}{2.303R}\left(\frac{298.15}{T} - 1 - 2.303 \times \log_{10}\frac{298.15}{T}\right) + \log_{10}K_{p2,25C}$	7.198	$\gamma_1\frac{K_{p2}}{\gamma_2}$
	$HPO_4^{2-} \rightleftharpoons PO_4^{3-} + H^+$ $\log_{10}K_{p3} = \frac{\Delta H_r^\circ}{2.303R}\left(\frac{1}{298.15} - \frac{1}{T}\right) + \frac{\Delta C_p^\circ}{2.303R}\left(\frac{298.15}{T} - 1 - 2.303 \times \log_{10}\frac{298.15}{T}\right) + \log_{10}K_{p3,25C}$	12.35	$\gamma_2\frac{K_{p3}}{\gamma_3}$
Orthosilicate (Busey & Mesmer, 1977; Nordstrom et al., 1990) (Volosov et al., 1972)	$H_4SiO_4 \rightleftharpoons H_3SiO_4^- + H^+$ $\log_{10}K_{s1} = -302.3724 - 0.05069842 \times T + \frac{15,669.69}{T} + 108.18466 \times \log_{10}T - \frac{1,119,669}{T^2}$	9.83	$\frac{K_{s1}}{\gamma_1}$
	$H_3SiO_4^- \rightleftharpoons H_2SiO_4^{2-} + H^+$ $\log_{10}K_{s2} = 8.354 - 0.021962 \times T - \frac{4,465.2}{T}$	13.17	$\gamma_1\frac{K_{s2}}{\gamma_2}$
Water (Nordstrom et al., 1990)	$H_2O \rightleftharpoons OH^- + H^+$ $\log_{10}K_w = -283.971 - 0.05069842 \times T + \frac{13,323}{T} + 102.24447 \times \log_{10}T - \frac{1,119,669}{T^2}$	14.000	K_w

[a]Equilibrium uses concentrations for chemical species, except for H^+ and OH^- which use activity. Correction for ionic strength for water equilibrium is not required as H^+ and OH^- activities are implemented in the buffer intensity equation for the water term (Equation 6c, $\beta_{w,IS}$). The activity of chemical i ($\{i\}$) having charge z (γ_z) is related to the molar concentration of chemical i ([i]) as $\{i\} = \gamma_z[i]$. Activity coefficients (γ_1, γ_2, and γ_3) are determined as per Equation 13.
[b]Refer to Table 3 for standard molar enthalpy change of the reaction $\left(\Delta H_r^\circ\right)$ and standard molar heat capacity change of the reaction $\left(\Delta C_p^\circ\right)$ values.

Chemical concentration inputs for the BIS are required in typical drinking water concentration units (e.g., mg C/L, mg N/L, or mg Cl_2/L) that are subsequently converted to molar concentrations for use in the buffer intensity simulations. For practical reasons, concentration units other than those that might be expected are used in two instances. First, for free bromine, the unit for concentration input is mg Cl_2/L (not mg Br_2/L) as mg Cl_2/L will be the typical unit provided from common drinking water wet chemistry methods such as *N*,*N*-diethyl-p-phenylenediamine (DPD) free and total chlorine methods (Hach Company, 2023b, 2023c). Second, for orthosilicate, the input units are mg silica (SiO_2)/L as that will be the typical units provided by common methods such as the silicomolybdate method (Hach Company, 2023a).

Note that certain disinfectant chemical species will not coexist in drinking water at measurable concentrations for any meaningful amount of time. For example, if free ammonia is measurable, then free bromine and free chlorine will not exist at measurable concentrations (Jafvert & Valentine, 1992; Wajon & Morris, 1982). To exclude a given chemical species from inclusion in the buffer intensity simulation (e.g., when the chemical is known not to be present), set the chemical concentration to zero.

2.3 | Equilibrium constants

To calculate the equilibrium constant (K) at the desired temperature in Kelvin (T), equilibrium constant equations were selected from the literature (Table 2). Depending on the equilibrium, the literature reported equilibrium constant equation was represented by one of three general equation types where each equation type corresponds to different assumptions regarding how the underlying thermodynamic parameters [i.e., standard molar enthalpy change of the reaction (ΔH_r°) and standard molar heat capacity change of the reaction (ΔC_p°)] vary with temperature.

The first equation type corresponds to both ΔH_r° and ΔC_p° varying with temperature (Equations 7a–7b). In Equations 7a–7b, A1–A5 are constants where either all five (Equation 7a; carbonate, first orthosilicate equilibrium, and water) or only the first three (Equation 7b; second orthosilicate equilibrium, free ammonia, and free chlorine) constants were reported in the literature. The differing number of constants corresponds to how ΔC_p° is assumed to vary with temperature where five (Equation 7a) and three (Equation 7b) constants represent ΔC_p° varying nonlinearly or linearly with temperature, respectively (Ramette, 1977; Stumm & Morgan, 1996).

$$\log_{10}K = A_1 + A_2 \times T + \frac{A_3}{T} + A_4 \times \log_{10}T - \frac{A_5}{T^2} \quad (7a)$$

$$\log_{10}K = A_1 + A_2 \times T + \frac{A_3}{T} \quad (7b)$$

The second equation type corresponds to ΔH_r° varying with temperature while ΔC_p° is temperature independent (Equation 8; orthophosphate), and the third equation type corresponds to ΔH_r° being temperature independent (Equation 9; free bromine), resulting in the van't Hoff equation. In Equations 8 and 9, R is the universal gas constant (8.314×10^{-3} kJ·K^{-1}·mol^{-1}), K_{25C} is the reported equilibrium constant at 25°C (298.15 K) and 0 M ionic strength (Table 2), and ΔH_r° (Equations 8 and 9) and ΔC_p° (Equation 8) are per the literature and provided in Table 3.

$$\log_{10}K = \frac{\Delta H_r^\circ}{2.303R}\left(\frac{1}{298.15} - \frac{1}{T}\right) + \frac{\Delta C_p^\circ}{2.303R}\left(\frac{298.15}{T} - 1 - 2.303 \times \log_{10}\frac{298.15}{T}\right) + \log_{10}K_{25C} \quad (8)$$

$$\log_{10}K = \frac{\Delta H_r^\circ}{2.303R}\left(\frac{1}{298.15} - \frac{1}{T}\right) + \log_{10}K_{25C} \quad (9)$$

TABLE 3 Summary of required thermodynamic information for the free bromine and orthophosphate equilibrium constant equations shown in Table 2.

System	Equilibrium constant	ΔH_r° (kJ·mol^{-1})	ΔC_p° (kJ·K^{-1}·mol^{-1})	Reference
Free Bromine	K_{br}	18.9	N/A	Benjamin (2015)[a]
Orthophosphate	K_{p1}	−8.0	−0.141	Goldberg et al. (2002)
	K_{p2}	3.6	−0.230	Goldberg et al. (2002)
	K_{p3}	16.0	−0.242	Goldberg et al. (2002)

ΔC_p°—standard molar heat capacity change of the reaction; ΔH_r°—standard molar enthalpy change of the reaction; N/A—not applicable.
[a]$\Delta H_r^\circ = H_{f,OBr^-}^\circ + H_{f,H^+}^\circ - H_{f,HOBr}^\circ$; H_{f,OBr^-}° (hypobromite ion heat of formation) = − 94.1 kJ·mol^{-1}; H_{f,H^+}° (hydrogen ion heat of formation) = 0 kJ·mol^{-1}; $H_{f,HOBr}^\circ$ (hypobromous acid heat of formation) = − 113.0 kJ·mol^{-1}.

The first orthosilicate equilibrium and equilibrium constant (K_{s1}) equation requires a further explanation to clarify how they were presented in the source literature and adjusted to the presentation in Table 2. For K_{s1}, Busey and Mesmer (1977) defined the first orthosilicate equilibrium as Equation 10 with an equation for their equilibrium constant (K_{BM}) that reduces to Equation 11 if a base 10 logarithm is used instead of a natural logarithm and ionic strength is assumed to be 0 M. Adding the water dissociation equilibrium to Equation 10 and water dissociation equilibrium constant equation (K_w) to Equation 11, as shown in Equation 12, results in the K_{s1} equilibrium and equilibrium constant equation presented in Table 2.

$$H_4SiO_4 + OH^- \rightleftharpoons H_3SiO_4^- + H_2O \tag{10}$$

$$\log_{10}K_{BM} = -18.4014 + \frac{2{,}346.69}{T} + 5.94019 \times \log_{10}T \tag{11}$$

$$\log_{10}K_{s1} = \log_{10}K_{BM} + \log_{10}K_w \tag{12}$$

2.4 | Ionic strength corrections

To account for the impact of ionic strength on equilibrium chemical concentrations, concentration-based equilibrium constants (K_{IS}) are calculated. The user-selected ionic strength in mM is converted to M and used to calculate required activity coefficients (γ_z) from the Davies equation, using Equation 13 (Benjamin, 2015; Davies, 1938; Davies, 1962) where z is the ion charge and μ is ionic strength in M. In Equation 13, the Debye–Hückel constant (A_{DH}) is determined from Equation 14 at the specified temperature in Kelvin (T) (Benjamin, 2015; Debye & Hückel, 1923; Zemaitis Jr. et al., 1986), and in Equation 15, the dielectric constant for water (ε_{water}) is determined at the specified temperature in °C (T_c) (Malmberg & Maryott, 1956). Using the determined γ_z, the concentration-based equilibrium constants (K_{IS}) are calculated as per Table 2.

$$\log_{10}\gamma_z = -A_{DH}\left(z^2\right)\left(\frac{\sqrt{\mu}}{1+\sqrt{\mu}} - 0.3\mu\right) \tag{13}$$

$$A_{DH} = 1.82 \times 10^6 \left(\varepsilon_{water} \times T\right)^{-3/2} \tag{14}$$

$$\varepsilon_{water} = 87.740 - 0.40008 \times T_c + 9.398 \times 10^{-4} \times {T_c}^2 - 1.410 \times 10^{-6} \times {T_c}^3 \tag{15}$$

2.5 | Optional inputs to estimate ionic strength and DIC

For ionic strength and DIC, alternative concentration input options have been provided. In lieu of entering a known ionic strength in mM, total dissolved solids (TDS, mg/L) or electrical conductivity (EC, µS/cm or µmho/cm) can be entered, and an estimated molar ionic strength (μ in M) will be calculated as per Equations 16 (Langelier, 1936) or 17 (Russell, 1976), respectively, and used for ionic strength corrections (Tchobanoglous et al., 2003).

$$\mu = 2.5 \times 10^{-5} \times TDS \tag{16}$$

$$\mu = 1.6 \times 10^{-5} \times EC \tag{17}$$

In lieu of entering a known DIC concentration, information about a total alkalinity water sample can be entered. The required inputs of the total alkalinity water sample are the measured temperature and pH at the time of the total alkalinity sample analysis and the resulting measured total alkalinity (TA) concentration of the water sample in mg/L as $CaCO_3$. Preferably, the total alkalinity measurement is performed using titration to the carbonic acid equivalence point rather than a fixed pH, which is inherently biased and can sometimes substantially under- or overestimate DIC (Weber & Stumm, 1964, 1963). Then, an estimate of the molar DIC concentration is calculated from the definition of total alkalinity as per Equation 18 (Benjamin, 2015), assuming that total alkalinity is only resulting from DIC and water (i.e., no other weak acids or weak bases are meaningful buffers). In Equation 18, the two α values (α_1 and α_2) are from the carbonate system equilibria for HCO_3^- and CO_3^{2-}, respectively, and α calculations use the temperature and pH specific to the total alkalinity water sample along with the ionic strength entered for the buffer intensity simulation. The subscript "init" for variables in Equation 18 indicates that these variables ($[H^+]$, $[OH^-]$, α_1, and α_2) are calculated using the total alkalinity water sample initial pH before titrating the water sample to determine total alkalinity. Finally, 50,000 in Equation 18 is the unit conversion to take TA from mg/L as $CaCO_3$ to equiv/L.

$$[DIC] = \frac{\frac{TA}{50{,}000} + [H^+]_{init} - [OH^-]_{init}}{(\alpha_1 + 2\alpha_2)_{init}} \tag{18}$$

It is possible that the inputted water chemistry parameters (pH, temperature, ionic strength, and total alkalinity) will estimate a chemically impossible, negative DIC concentration likely associated with the analytical

uncertainty in the measured, input parameters and/or the assumption that only DIC and water are contributing to total alkalinity. Therefore, if a negative DIC concentration is estimated, the BIS notes that a chemically impossible condition has been inputted and sets the estimated DIC concentration to zero.

2.6 | Strong acid or strong base addition to change pH

The area under a total buffer intensity curve between two pH values represents the required addition of strong acid or strong base to lower or raise the pH, respectively, from one pH value to the other. For a given total buffer intensity curve, the BIS allows the user to select two pH values, and the BIS calculates and reports the required addition of strong acid or strong base in milliequivalent/L to change the pH between the two selected pH values. The area under the total buffer intensity curve between the two pH values of interest is estimated by the trapezoid rule, using the total buffer intensity values that are calculated every 0.01 pH units. Note that, by definition, strong base or strong acid addition assumes no change in the underlying weak acid or weak base concentrations (or ionic strength) such that only a pH change occurs with no change to the total buffer intensity curve (e.g., DIC does not change).

2.7 | Buffer intensity simulator code and graphical user interface

Instructions for acquiring and running the BIS are provided in the Supporting Information (*Instructions for Acquiring and Running BIS R Code*). Running the BIS provides a locally running interactive application for the user to simulate buffer intensity curves, containing a graphical user interface developed using the R Shiny package (Chang et al., 2024). The graphical user interface allows interactive selection of simulation conditions and buffer intensity curve generation. Furthermore, the simulation results and initial conditions are exportable as comma seperated variable (.csv) files, and buffer intensity curves are exportable as portable network graphic (.png) files. A detailed description of the graphical user interface is provided in the Supporting Information (*Graphical User Interface Description*).

2.8 | Model verification

To verify BIS implementation, 551 individual water chemistry conditions (pH 4.5 to 10.0 in 0.01 pH increments, 35°C, 100 mM ionic strength, 10 mg C/L DIC, 10 mg N/L free ammonia, 10 mg Cl_2/L free bromine, 10 mg Cl_2/L free chlorine, 10 mg orthophosphate/L, and 50 mg silica/L orthosilicate) were simulated with the BIS and compared to identical calculations performed in Microsoft Excel. Calculated buffer intensity for each of the seven chemical species (water, carbonate, orthophosphate, orthosilicate, free ammonia, free bromine, and free chlorine) and the total buffer intensity were numerically identical between all ($n = 4408$) BIS and Microsoft Excel simulated conditions. Therefore, the BIS implementation was numerically verified.

3 | PRACTICAL APPLICATION SIMULATIONS

The BIS was used to conduct simulations for three practical and sometimes encountered drinking water scenarios to illustrate the utility of using the BIS to simulate drinking water buffer intensity: (1) carbonate (i.e., DIC) importance, (2) temperature impacts, and (3) nitrification resulting from the presence of free ammonia from chloramine use and/or free ammonia source water presence.

3.1 | Carbonate buffered drinking water

DIC is present in all drinking waters to some extent and is typically an important (if not the main) contributor to total buffer intensity, and DIC concentration can be changed by treatment processes (e.g., lime softening, recarbonation, and caustic addition). Therefore, an example drinking water condition (25°C, 5 mM ionic strength, 3 mg orthophosphate/L, and 2 mg Cl_2/L free chlorine) with three different DIC concentrations (1, 10, and 50 mg C/L DIC) were simulated (Figures 1 and 2) and are used to illustrate several points related to buffer intensity: (1) the general total buffer intensity curve shape when (i) one or (ii) multiple weak acid systems are major contributors to total buffer intensity, (2) the impact of total weak acid concentration changes when (i) one or (ii) multiple weak acid systems are major contributors to total buffer intensity, and (3) utility of total buffer intensity curves to calculate the (i) strong acid or strong base addition required to change a given water between two pH values or (ii) relative resistance of a given water to a specific pH change.

As noted previously, a total buffer intensity curve is a summation of each of the underlying individual weak acid system buffer intensity curves. For the two greater DIC concentrations (10 and 50 mg C/L) simulated in Figure 1, DIC is the major contributor to total buffer

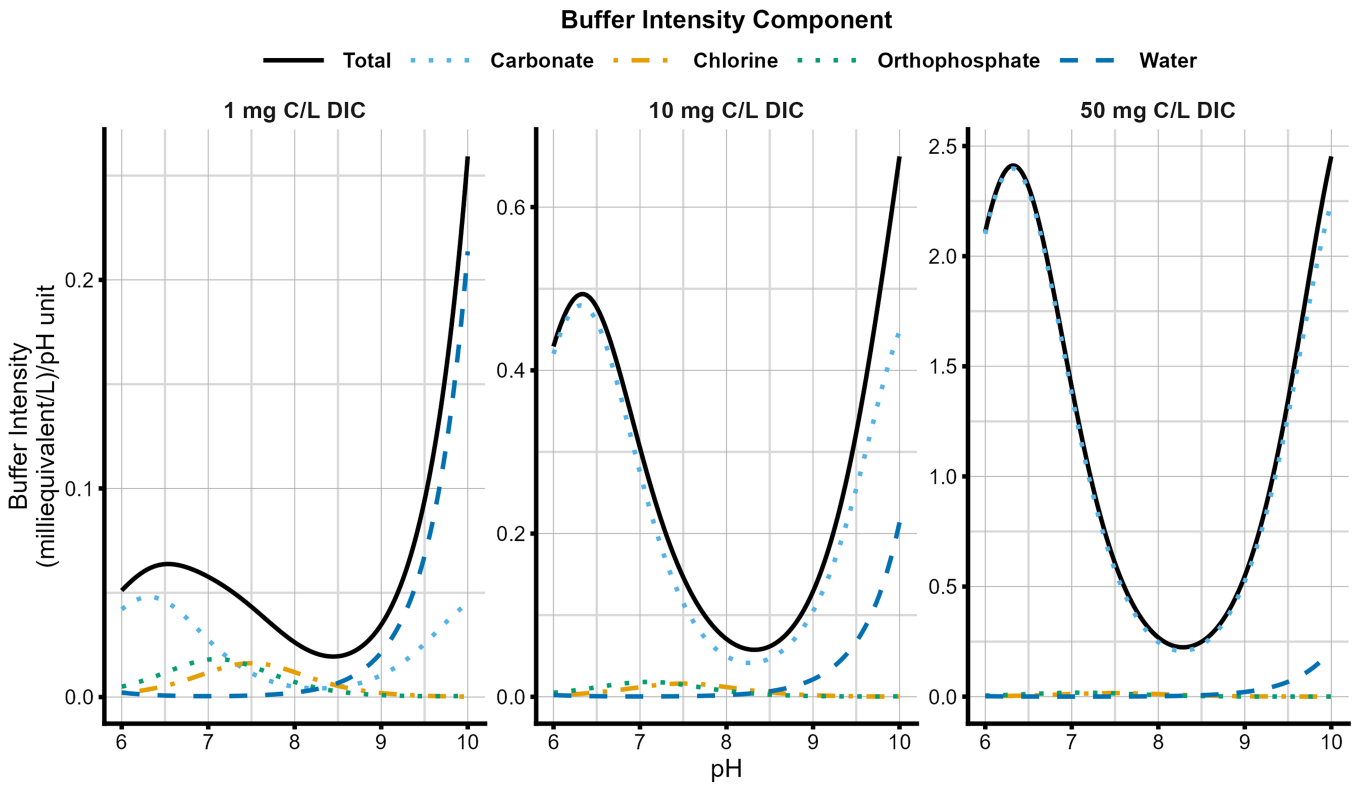

FIGURE 1 Impact of dissolved inorganic carbon (DIC) concentration on simulated buffer intensity (25°C, 5 mM ionic strength, 3 mg orthophosphate/L, and 2 mg Cl_2/L free chlorine). Total = sum of individual components, Carbonate = carbonate system (i.e., DIC), Chlorine = free chlorine system, Orthophosphate = orthophosphate system, and Water = water system.

intensity from pH 6 to 10. Therefore, the resulting total buffer intensity curve displays characteristics typical of a single weak acid system (i.e., carbonate) where peaks (local maximums in total buffer intensity) occur when pH equals a pK value and valleys (local minimums in total buffer intensity) occur when pH equals the average of two successive pK values. Thus, total buffer intensity curve peaks for the 10 and 50 mg C/L simulations (Figure 1) occur where pH is equal to the carbonate first dissociation pK (pH = 6.3 for 25°C and 5 mM ionic strength), and a total buffer intensity curve valley occurs where the pH is equal to the average of the two carbonate dissociation pK values (pH = 8.3 for 25°C and 5 mM ionic strength). Alternatively, the 1 mg C/L DIC concentration simulation (Figure 1) represents a weaker buffered water where the weak acid system that is the major contributor to the total buffer intensity varies by pH; therefore, the total buffer intensity curve is impacted by all the underlying weak acid system buffer intensity curves. Specifically, below pH 7.2, DIC is the major contributor to total buffer intensity (Carbonate, Figure 1). Between pHs 7.2 and 8.5, orthophosphate (Orthophosphate, Figure 1) and free chlorine (Chlorine, Figure 1) are the major contributors to total buffer intensity, corresponding to being within a pH unit of their respective pK values (7.1 and 7.5, respectively, for 25°C and 5 mM ionic strength). Above pH 8.5, water becomes the major contributor to total buffer intensity and constitutes essentially all the total buffer intensity as pH increases.

Figures 1 and 2 also illustrate the impact to buffer intensity when changing one (i.e., carbonate) of the total weak acid concentrations. For the 10 and 50 mg C/L DIC concentration simulations, DIC is the major contributor to total buffer intensity. Therefore, the relative total buffer intensity between the two simulations at any pH is proportional to the two DIC concentrations, increasing by an approximate factor of five for a factor of five increase in DIC concentration (10 to 50 mg C/L). The proportionality to DIC concentration is expected based on the buffer intensity calculations (e.g., Equations 3–5) where each component of total buffer intensity is proportional to the total concentration of the given weak acid system, and in these cases (10 to 50 mg C/L DIC), a single weak acid system (carbonate) dominates. When multiple weak acid systems are major contributors to total buffer intensity, the corresponding increase in total buffer intensity is not directly proportional to the DIC concentration increase. At pH 7.5 and 1 mg C/L DIC (Figure 1), DIC, orthophosphate, and free chlorine are all important contributors (0.012, 0.015, and 0.016 (milliequivalent/L)/pH

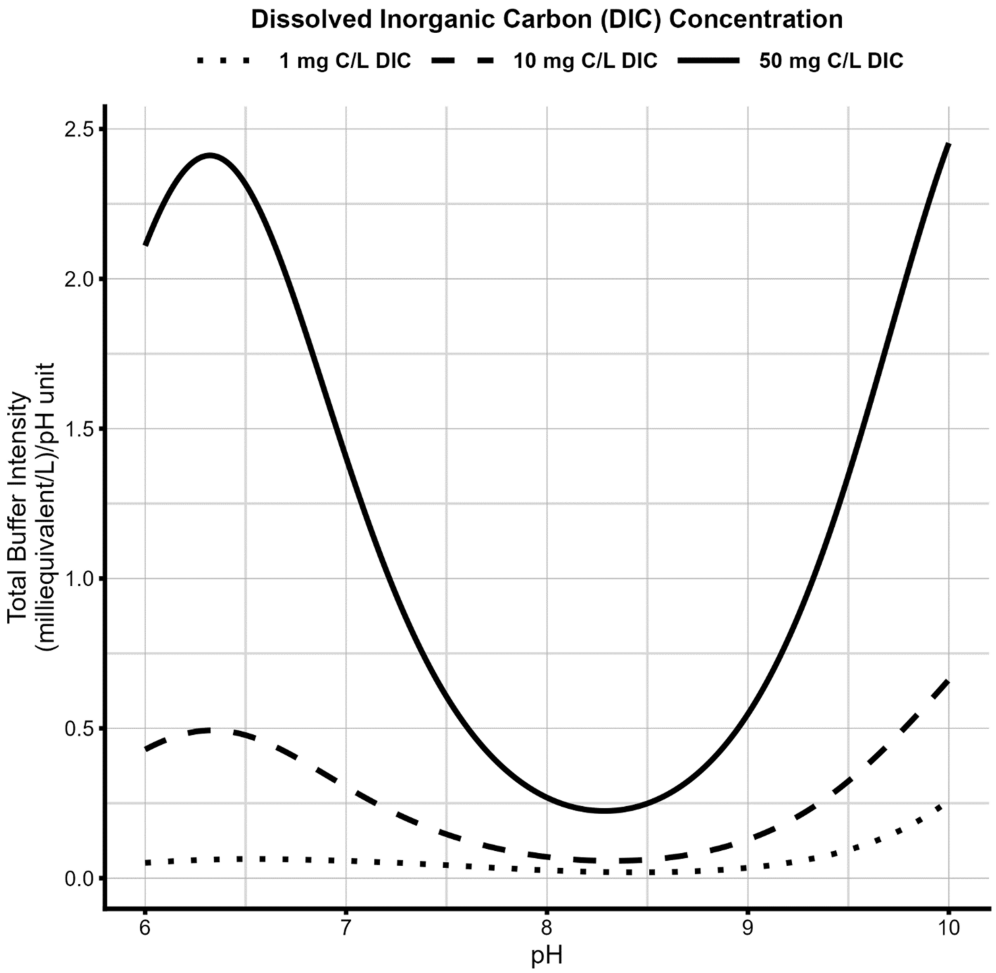

FIGURE 2 Simulated total buffer intensity (25°C, 5 mM ionic strength, 3 mg orthophosphate/L, and 2 mg Cl_2/L free chlorine) for various dissolved inorganic carbon (DIC) concentrations. Figure data for the three simulations were exported from the buffer intensity simulator (BIS) as comma seperated variable (.cvs) files and replotted here (see Supporting Information *Graphical User Interface Description* for details on exporting data from BIS simulations for external use).

unit, respectively) to the 0.043 (milliequivalent/L)/pH unit total buffer intensity; therefore, unlike the case where DIC is the dominant contributor to total buffer intensity, a DIC concentration increases by a factor of 10 (1 to 10 mg C/L) only leads to an increase in total buffer intensity by a factor of 3.5.

A practical value that can be obtained from total buffer intensity curves is how much strong acid or strong base would be required to change the pH to a new value (i.e., the area under the curve between the two selected pH values). For instance, if a utility was considering changing their operating pH from 7.2 to 8.5, the total buffer intensity curves in Figures 1 and 2 represent the impact of various DIC concentrations on assessing the amount of chemical required to make the pH change. The strong base required to raise the pH is estimated as 0.042, 0.14, and 0.56 milliequivalent/L for the 1, 10, and 50 mg C/L DIC simulations, respectively, and the relative strong base additions are factors of 3.3 (10 vs. 1 mg C/L DIC), 4.0 (50 vs. 10 mg C/L DIC), and 13 (50 vs. 1 mg C/L DIC). Alternatively, if no orthophosphate or free chlorine were present in the water (i.e., only including the *Carbonate* and *Water* contributions to buffer intensity shown in Figure 1), the required strong base additions for a pH change from 7.2 to 8.5 decreases to 0.013, 0.11, and 0.53 milliequivalent/L for the 1, 10, and 50 mg C/L DIC simulations, respectively. The corresponding relative strong base additions are now factors of 8.5 (10 vs. 1 mg C/L DIC), 4.8 (50 vs. 10 mg C/L DIC), and 41 (50 vs. 1 mg C/L DIC). Because only DIC (besides water) is now present to provide buffer intensity, the relative strong base additions approach the relative DIC concentrations.

A final practical example from Figures 1 and 2 is how much strong acid or strong base would be required to decrease or increase the pH by 0.5 units when operating at a peak (i.e., pH 6.3) versus a valley (i.e., pH 8.3) in the total buffer intensity curve, illustrating the relative stability of operating at the two pH values. For the 10 mg C/L DIC concentration simulation in Figure 1, the total buffer intensity is 0.49 and 0.058 (milliequivalent/L)/pH unit at pHs 6.3 and 8.3, respectively. To change the pH from 6.3 by 0.5 pH units, approximately 0.22 milliequivalent/L of strong acid (decrease to pH 5.8) or strong base (increase to pH 6.8) are required, but for pH 8.3, only 0.035 milliequivalent/L of strong acid or strong base is required to decrease or increase the pH by 0.5 units, respectively.

Therefore, only 16% of the strong acid or strong base is required at pH 8.3 versus pH 6.3 to induce a 0.5 pH unit change. Furthermore, if the 0.035 milliequivalent/L strong base or strong acid required to change the pH by 0.5 units at pH 8.3 were added to the pH 6.3 condition, the pH would change by less than 0.1 pH units.

3.2 | Temperature impact

Distributed water temperature may vary seasonally and through distribution. As all equilibria included in the BIS vary with temperature (Table 2), buffer intensity calculations are temperature dependent. Figure 3 illustrates the impact of temperature (5, 20, or 35°C) on a buffer intensity simulation where only DIC is assumed to be present and at a relatively low concentration (5 mg C/L DIC and 0 mM ionic strength); therefore, only water and carbonate are contributing to the total buffer intensity curves. The major temperature impact to the total buffer intensity curve is associated with water providing the greatest buffer intensity at relatively high pH values (e.g., pH >9). The increased water contribution to total buffer intensity results from an order of magnitude increase in the water dissociation constant (K_w) from 5°C (1.85×10^{-15}) to 35°C (2.05×10^{-14}). Specifically, the contribution of hydroxide ion (OH^-) to total buffer intensity increases in direct proportion to changes in K_w (Equation 6b). Conversely, the two carbonate equilibrium constants (K_{c1} and K_{c2}) only increase by factors of 1.6 and 2.0, respectively, from 5°C (3.05×10^{-7} K_{c1} and 2.79×10^{-11} K_{c2}) to 35°C (4.89×10^{-7} K_{c1} and 5.60×10^{-11} K_{c2}), resulting in minor changes in the carbonate system contribution to total buffer intensity.

Assuming the pH is 9.5 (Figure 3), water goes from being a minor contributor to total buffer intensity at 5°C (16% of total buffer intensity) to being the dominant contributor to total buffer intensity at 35°C (55% of total buffer intensity). Furthermore, comparing the 5 and 35°C simulations at pH 9.5 (Figure 3), the total buffer intensity increases by a factor of three from 0.086 to 0.27 (milliequivalent/L)/pH unit. Likewise, the amount of strong acid or strong base required to change the pH by 0.5 pH units also increases by approximately a factor of three when going from 5 to 35°C for both a 0.5 pH unit decrease (0.027 to 0.086 milliequivalent/L) or increase (0.070 to 0.23 milliequivalent/L). Together, the simulation highlights how temperature (e.g., seasonality) impacts the ability of a low DIC (5 mg C/L) and high pH (pH >9) water to resist pH changes which implies that chemical feed rates for pH adjustment (e.g., as a corrosion control treatment) may need to be seasonally adjusted. Finally, for drinking water

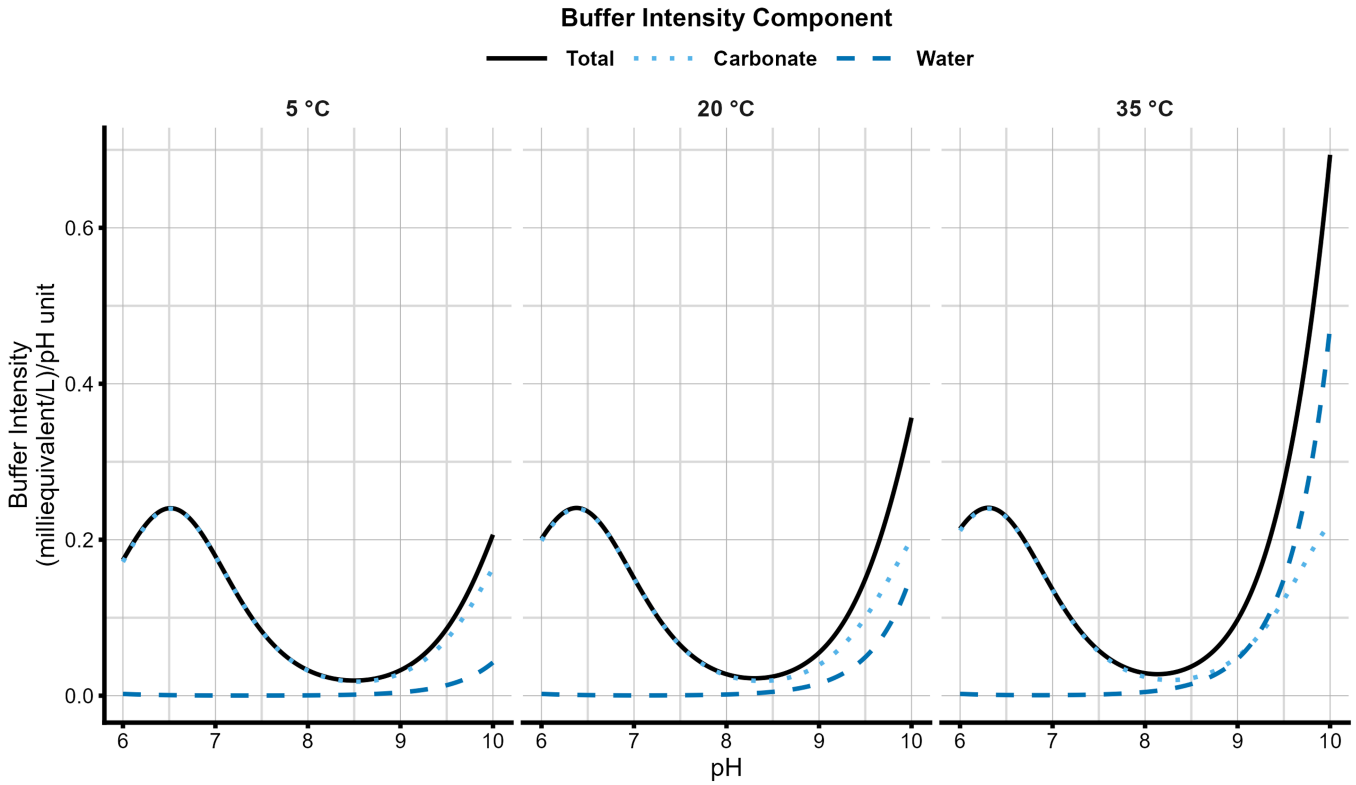

FIGURE 3 Impact of temperature on simulated buffer intensity (0 mM ionic strength and 5 mg C/L dissolved inorganic carbon). Total = sum of individual components, Carbonate = carbonate system (i.e., DIC), and Water = water system.

where typical pHs range from 6 to 10, Figure 3 illustrates that the water contribution to total buffer intensity is only relevant in weakly buffered waters at pHs greater than approximately 8.

3.3 | Free ammonia and nitrification considerations

Drinking water sources may contain free ammonia at elevated (e.g., >4 mg N/L) concentrations (Brandhuber, 2012; Keithley et al., 2021) that can be removed (at least partially) during treatment (Blute et al., 2012) from processes that include biological oxidation (Lytle et al., 2007; Lytle et al., 2015; Lytle et al., 2020), ion exchange (Keithley et al., 2021), or breakpoint chlorination (Henrie et al., 2012). If not completely removed during treatment, some of the free ammonia will form chloramines upon free chlorine addition (Jafvert & Valentine, 1992), leaving the remaining free ammonia in the water during distribution. In some cases, the finished water free ammonia concentration can reach concentrations well above (i.e., >4 mg N/L) what would be considered typical (i.e., <0.5 mg N/L) when using chloramines as a secondary disinfectant (American Water Works Association, 2013; Keithley et al., 2021). Furthermore, it is common for chloramine systems to operate at elevated pHs (i.e., > pH 8) to promote chloramine stability, and the availability of free ammonia provides the opportunity for biological nitrification to occur in the distribution system which will also consume DIC (American Water Works Association, 2013).

Figure 4 illustrates the impact of varying free ammonia concentrations on total buffer intensity (20°C, 0 mM ionic strength, and 10 mg C/L DIC), spanning from a practical maximum free ammonia concentration (0.5 mg N/L) in chloramine systems without source water free ammonia to cases where source water free ammonia leads to elevated free ammonia concentrations (2 and 4 mg N/L) in finished waters. For the 0.5 mg N/L free ammonia simulation, carbonate remains the major buffer and free ammonia presence minimally increases total buffer intensity. As free ammonia concentration increases, free ammonia does become impactful to total buffer intensity around the free ammonia pK (i.e., pH 9.4), and at pH 9.5, an increase in free ammonia from 0.5 to 4 mg N/L increases total buffer intensity by 50% (0.27 to 0.41 (milliequivalent/L)/pH unit).

If free ammonia is present from the source water or from making chloramines, nitrification may occur. Complete nitrification where free ammonia is oxidized to

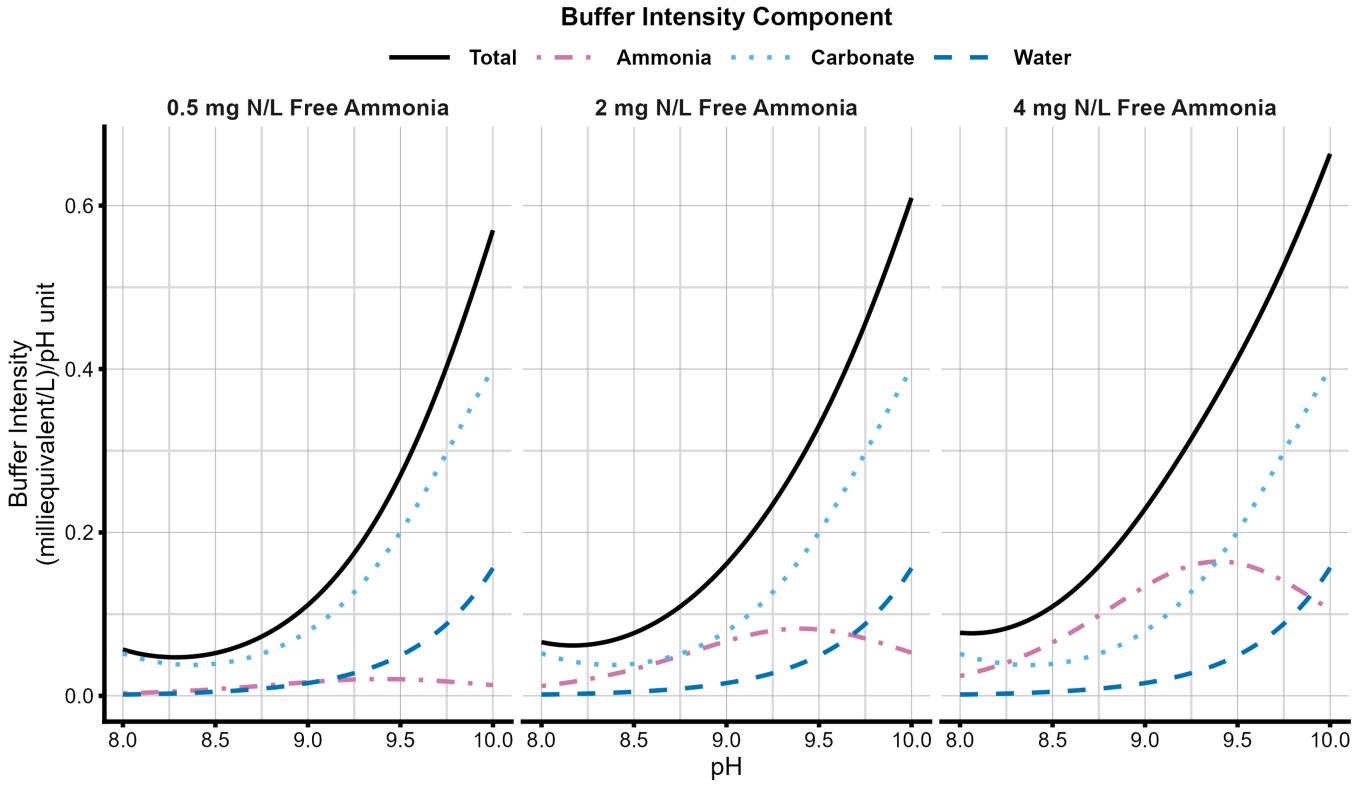

FIGURE 4 Impact of free ammonia on simulated buffer intensity (20°C, 0 mM ionic strength, and 10 mg C/L dissolved inorganic carbon). Total = sum of individual components, Ammonia = free ammonia system, Carbonate = carbonate system (i.e., DIC), and Water = water system.

nitrate can be represented by Equation 19 and results in free ammonia, alkalinity, dissolved oxygen, and DIC decreasing (Tchobanoglous et al., 2003). For each mg N/L of ammonia consumed per Equation 19, 7.1 mg/L as $CaCO_3$ of alkalinity is removed, 4.3 mg/L of dissolved oxygen is consumed, and 0.08 mg C/L of DIC are incorporated into new cells ($C_5H_7O_2N$). Therefore, nitrification will slightly decrease DIC, decrease dissolved oxygen, and depending on buffer intensity, could decrease pH to a large extent. An important point is that when free ammonia is an important contributor to total buffer intensity, nitrification has two impacts. First, nitrification effectively introduces an acid (Equation 19) into the water. Second, nitrification directly removes the free ammonia component from total buffer intensity (i.e., decreasing free ammonia [TOTA]), allowing continued nitrification to impact the water to a greater extent than expected from the first effect alone.

$$NH_3 + 1.863O_2 + 0.098CO_2 \rightarrow 0.0196C_5H_7O_2N + 0.98NO_3^- + 0.0941H_2O + 0.98H^+ \quad (19)$$

For an initial pH of 9.0 (Figure 4) and assuming 0.5 mg N/L of free ammonia is oxidized to nitrate by nitrification and the total chlorine concentration is minimal, the resulting final pH is greater for conditions with greater buffer intensity provided by the increasing initial free ammonia concentrations of 0.5 mg N/L (final pH 7.9), 2 mg N/L (final pH 8.4), and 4 mg N/L (final pH 8.7). Although the example illustrates greater buffer intensity from greater initial free ammonia concentrations, nitrification would likely continue for the two greater initial free ammonia concentrations (2 and 4 mg N/L) until becoming dissolved oxygen limited after consuming approximately 2 mg N/L free ammonia, using 8.6 mg/L dissolved oxygen. Accounting for this scenario, the resulting final pHs further decrease to 6.9 and 7.0 for the initial 2 and 4 mg N/L free ammonia concentrations, respectively, resulting in a pH that is approximately 1 unit lower than for the 0.5 mg N/L initial free ammonia concentration condition.

4 | SUMMARY

The developed open-source BIS is freely available for download and can be used to simulate buffer intensity for user-selected water quality conditions. A practical value that can be obtained from total buffer intensity curves is how much strong acid or strong base would be required to change the pH to a new value (i.e., the area under the curve between the two selected pH values). Using the BIS, simulations were conducted to illustrate impacts to buffer intensity for three practical drinking water scenarios, including the impact of DIC concentration, temperature, and free ammonia concentration. Overall, BIS provides a tool to allow drinking water practitioners to simulate buffer intensity for their specific water quality. Finally, the code is open source; therefore, it can be modified as per user requirements and/or incorporated into other analyses.

AUTHOR CONTRIBUTIONS

David G. Wahman: Conceptualization; data curation; software; formal analysis; validation; investigation; visualization; methodology; writing – original draft; project administration; writing – review and editing. **Michael R. Schock:** Conceptualization; investigation; methodology; writing – original draft; writing – review and editing. **Darren A. Lytle:** Conceptualization; investigation; writing – original draft; writing – review and editing.

ACKNOWLEDGMENTS

This work has been subjected to the United States Environmental Protection Agency's (Agency's) review and has been approved for publication. The views expressed in this manuscript are those of the authors and do not necessarily represent the views or policies of the Agency. Any mention of trade names, products, or services does not imply an endorsement by the Agency. The Agency does not endorse any commercial products, services, or enterprises.

CONFLICT OF INTEREST STATEMENT

The authors have no conflict of interest to declare.

DATA AVAILABILITY STATEMENT

The data appearing in this publication can be generated using the BIS and are also available on the EPA's Science Hub at https://catalog.data.gov/dataset/.

ORCID

David G. Wahman https://orcid.org/0000-0002-0167-8468

Michael R. Schock https://orcid.org/0000-0001-9248-6690

Darren A. Lytle https://orcid.org/0000-0002-5282-4541

REFERENCES

American Water Works Association. (2013). *Nitrification prevention and control in drinking water (AWWA manual M56)* (2nd ed.). American Water Works Association.

Bates, R. G., & Pinching, G. D. (1949). Acidic dissociation constant of ammonium ion at 0° to 50°C, and the base strength of ammonia. *Journal of Research of the National Bureau of Standards*, *42*, 419. https://doi.org/10.6028/jres.042.037

Benjamin, M. M. (2015). *Water chemistry* (2nd ed.). Waveland Press, Inc.

Benjamin, M. M., Sontheimer, H., & Leroy, P. (1996). Chapter 2 – Corrosion of iron and steel. In *Internal corrosion of water distribution systems* (2nd ed.). American Water Works Association Research Foundation.

Blute, N., Ghosh, A., & Lytle, D. (2012). Assessing ammonia treatment options. *Opflow*, *38*(5), 14. https://doi.org/10.5991/OPF.2012.38.0025

Brandhuber, P. J. (2012). What's your ammonia IQ? *Opflow*, *38*(4), 12–14. https://doi.org/10.5991/OPF.2012.38.0021

Busey, R. H., & Mesmer, R. E. (1977). Ionization equilibriums of silicic acid and Polysilicate formation in aqueous sodium chloride solutions to 300°C. *Inorganic Chemistry*, *16*(10), 2444–2450. https://doi.org/10.1021/ic50176a004

Butler, J. N. (1964). *Ionic equilibrium: A mathematical approach*. Addison-Wesley Publishing Company.

Butler, J. N., & Cogley, D. R. (1998). *Ionic equilibrium: Solubility and pH calculations*. John Wiley and Sons.

Chang, W., Cheng, J., Allaire, J., Sievert, C., Schloerke, B., Xie, Y., Allen, J., McPherson, J., Dipert, A., & Borges, B. (2024). Shiny: Web application framework for R. R package version 1.8.1.1.

Clement, J. A., Daly, W. J., Shorney, H. J., & Capuzzi, A. J. (1998). An Innovative Approach to Understanding and Improving Distribution System Water Quality. *Proceedings of AWWA Water Quality & Technology Conference*.

Clement, J. A., & Schock, M. R. (1998). Buffer Intensity: What Is It, and Why It's Critical for Controlling Distribution System Water Quality. *Proceedings of AWWA Water Quality & Technology Conference*.

Company, H. (2023a). *Method 8185, Silicomolybdate method, powder pillows, 1 to 100 mg/L SiO_2 (HR, spectrophotometers), 1 to 75 mg/L SiO_2 (HR, colorimeters)*. Hach Company.

Company, H. (2023b). *Method 10,260, free chlorine. USEPA DPD method, Chemkey reagents, 0.04 to 4.0 mg/L as Cl_2*. Hach Company.

Company, H. (2023c). *Method 10,260, Total chlorine. USEPA DPD method, Chemkey reagents, 0.04 to 10.0 mg/L as Cl_2*. Hach Company.

Davies, C. W. (1938). 397. The extent of dissociation of salts in water. Part VIII. An equation for the mean ionic activity coefficient of an electrolyte in water, and a revision of the dissociation constants of some sulphates. *Journal of the Chemical Society (Resumed)*:0, 2093. https://doi.org/10.1039/JR9380002093

Davies, C. W. (1962). *Ion association*. Butterworths.

Debye, P., & Hückel, E. (1923). The theory of electrolytes. I. Freezing point depression and related phenomena [Zur Theorie der Elektrolyte. I. Gefrierpunktserniedrigung und verwandte Erscheinungen] translated and typeset by Michael J. Braus (2020). *Physikalische Zeitschrift*, *24*, 185. http://digital.library.wisc.edu/1793/79225

Goldberg, R. N., Kishore, N., & Lennen, R. M. (2002). Thermodynamic quantities for the ionization reactions of buffers. *Journal of Physical and Chemical Reference Data*, *31*(2), 231–370. https://doi.org/10.1063/1.1416902

Henrie, T., Rezania, L.-I. W., Nagy, D., & Lytle, D. A. (2012). Got ammonia? *Opflow*, *38*(6), 22–24. https://doi.org/10.5991/OPF.2012.38.0033

Jafvert, C. T., & Valentine, R. L. (1992). Reaction scheme for the chlorination of ammoniacal water. *Environmental Science & Technology*, *26*(3), 577–586. https://doi.org/10.1021/es00027a022

Keithley, A. E., Muhlen, C., Wahman, D. G., & Lytle, D. A. (2021). Fate of ammonia and implications for distribution system water quality at four ion exchange softening plants with elevated source water ammonia. *Water Research*, *203*, 117485. https://doi.org/10.1016/j.watres.2021.117485

Kim, C. (2003). An aquatic chemistry spreadsheet for general chemistry classes. *Journal of Chemical Education*, *80*(11), 1351. https://doi.org/10.1021/ed080p1351.2

Langelier, W. F. (1936). The analytical control of anti-corrosion water treatment. *Journal AWWA*, *28*(10), 1500–1521. https://doi.org/10.1002/j.1551-8833.1936.tb13785.x

Loewenthal, R. E., & Marais, G.v. R. (1976). *Carbonate chemistry of aquatic systems: Theory and application*. Ann Arbor Science Publishers, Inc.

Lytle, D. A., Sorg, T. J., Wang, L., Muhlen, C., Rahrig, M., & French, K. (2007). Biological nitrification in a full-scale and pilot-scale iron removal drinking water treatment plant. *Journal of Water Supply Research and Technology-AQUA*, *56*(2), 125–136. https://doi.org/10.2166/aqua.2007.092

Lytle, D. A., Williams, D., Muhlen, C., Pham, M., Kelty, K., Wildman, M., Lang, G., Wilcox, M., & Kohne, M. (2015). The full-scale implementation of an innovative biological ammonia treatment process. *Journal AWWA*, *107*(12), E648. https://doi.org/10.5942/jawwa.2015.107.0176

Lytle, D. A., Williams, D., Muhlen, C., Riddick, E., & Pham, M. (2020). The removal of ammonia, arsenic, iron and manganese by biological treatment from a small Iowa drinking water system. *Environmental Science: Water Research & Technology*, *6*(11), 3142–3156. https://doi.org/10.1039/D0EW00361A

Malmberg, C. G., & Maryott, A. A. (1956). Dielectric constant of water from 0° to 100°C. *Journal of Research of the National Bureau of Standards*, *56*(1), 1. https://doi.org/10.6028/jres.056.001

Morris, J. C. (1966). The acid ionization constant of HOCl from 5 to 35°. *The Journal of Physical Chemistry*, *70*(12), 3798–3805. https://doi.org/10.1021/j100884a007

Nordstrom, D. K., Plummer, L. N., Langmuir, D., Busenberg, E., May, H. M., Jones, B. F., & Parkhurst, D. L. (1990). Revised chemical equilibrium data for major water—Mineral reactions and their limitations. In *Chemical modeling of aqueous systems II*. American Chemical Society.

Plummer, L. N., & Busenberg, E. (1982). The solubilities of calcite, aragonite and Vaterite in CO_2-H_2O solutions between 0 and 90°C, and an evaluation of the aqueous model for the system $CaCO_3$-CO_2-H_2O. *Geochimica et Cosmochimica Acta*, *46*(6), 1011–1040. https://doi.org/10.1016/0016-7037(82)90056-4

R Core Team. (2024). *R: A language and environment for statistical computing*. R Foundation for Statistical Computing.

Ramette, R. W. (1977). On deducing the pK-temperature equation. *Journal of Chemical Education*, *54*(5), 280. https://doi.org/10.1021/ed054p280

Russell, L. L. (1976). *Chemical aspects of groundwater recharge with wastewaters*. Dissertation. University of California, Berkeley.

Schock, M. R., & Lytle, D. A. (2011). Internal corrosion and deposition control. In *Water quality and treatment: A handbook of community water supplies*. McGraw-Hill, Inc.

Schock, M. R., Lytle, D. A., & Clement, J. A. (1995). Effect of pH, DIC, orthophosphate and sulfate on drinking water Cuprosolvency (EPA/600/R-95/085), Washington, DC.

Snoeyink, V. L., & Wagner, I. (1996). Chapter 1 – Principles of corrosion in water distribution systems. In *Internal corrosion of water distribution systems* (2nd ed.). American Water Works Association Research Foundation.

Stumm, W. (1960). Investigation of the corrosive behavior of waters. *Journal of the Sanitary Engineering Division*, *86*(6), 27–46. https://doi.org/10.1061/JSEDAI.0000306

Stumm, W., & Morgan, J. J. (1996). *Aquatic chemistry chemical equilibria and rates in natural waters*. Wiley.

Tchobanoglous, G., Burton, F. L., & Stensel, H. D. (2003). *Wastewater engineering: Treatment and reuse* (4th ed.). The McGraw-Hill Companies, Inc.

Urbansky, E. T., & Schock, M. R. (2000). Understanding, deriving, and computing Buffer capacity. *Journal of Chemical Education*, *77*(12), 1640. https://doi.org/10.1021/ed077p1640

USEPA. (2019). *Optimal corrosion control treatment evaluation technical recommendations for primacy agencies and public water systems (EPA 816-B-16-003, dated march 2016, updated 2019)*. United States Environmental Protection Agency.

Volosov, A. G., Khodakov, I. L., & Ryzhenko, B. N. (1972). Equilibrium in system SiO_2-H_2O at elevated temperatures along the lower three-phase curve. *Geochemistry International*, *9*, 362.

Wahman, D. G., Pinelli, M. D., Schock, M. R., & Lytle, D. A. (2021). Theoretical equilibrium Lead(II) solubility revisited: Open source code and practical relationships. *AWWA Water Science*, *3*(5), e1250. https://doi.org/10.1002/aws2.1250

Wajon, J. E., & Morris, J. C. (1982). Rates of formation of *N*-bromo amines in aqueous solution. *Inorganic Chemistry*, *21*(12), 4258–4263. https://doi.org/10.1021/ic00142a030

Weber, W. J., & Stumm, W. (1963). Mechanism of hydrogen ion buffering in natural waters. *Journal American Water Works Association*, *55*(12), 1553–1578. https://doi.org/10.1002/j.1551-8833.1963.tb01178.x

Weber, W. J., & Stumm, W. (1964). Correction – mechanism of hydrogen ion buffering in natural waters. *Journal American Water Works Association*, *56*(4), 386. https://doi.org/10.1002/j.1551-8833.1964.tb01223.x

Zemaitis, J. F., Jr., Clark, D. M., Rafal, M., & Scrivner, N. C. (1986). *Handbook of aqueous electrolyte thermodynamics*. John Wiley & Sons, Inc.

SUPPORTING INFORMATION

Additional supporting information can be found online in the Supporting Information section at the end of this article.

How to cite this article: Wahman, D. G., Schock, M. R., & Lytle, D. A. (2024). Drinking water buffer intensity simulator (BIS): Development and practical simulations. *AWWA Water Science*, *6*(6), e70006. https://doi.org/10.1002/aws2.70006